

MICROWAVE MEASUREMENTS OF GaAs INTEGRATED CIRCUITS USING ELECTROOPTIC SAMPLING

K. J. Weingarten, R. Majidi-Ahy, M. J. W. Rodwell, B.A. Auld, and D. M. Bloom

Edward L. Ginzton Laboratory
Stanford University
Stanford, CA 94305

Abstract

We describe the electrooptic sampling system at Stanford with emphasis on the requirements for microwave measurements. Results presented include internal-node measurements of 20 GHz distributed amplifiers, propagation delays in GaAs frequency dividers clocked to 18 GHz, and VSWR on IC transmission lines to 40 GHz.

Introduction

Gallium Arsenide (GaAs) microwave integrated circuits (IC's) now operate at millimeter-wave frequencies, while GaAs digital IC's operate with clock rates at microwave frequencies up to 18 GHz. Digital IC's are currently tested only by indirect techniques (multi-stage propagation delay or cycle times), while microwave circuits are tested by external scattering parameters; if the circuit does not perform correctly, the cause can only be inferred from its external response. Electrooptic sampling was initially developed to measure the response of photoconductors and photodetectors faster than the time resolution of sampling oscilloscopes and used an external electrooptic modulator connected to the device under test in a hybrid fashion [1,2]. The system developed at Stanford uses the GaAs IC substrate as the electrooptic material, permitting detailed internal-node circuit evaluation with picosecond time resolution.

The Sampling System

GaAs is electrooptic; the electric fields associated with conductor voltages induce optical birefringence, causing a polarization change to a probe beam passing through these fields. Figures 1 and 2 show the cross-section of typical probing geometries. For standard [100] cut GaAs substrates the probe beam polarization is affected only by the longitudinal field components. The beam is focused through the IC substrate where its polarization is modulated by the voltage across the substrate at the test point. The reflected light is passed through a polarizer and its intensity detected by a photodiode. The probe beam polarization is adjusted to the linear region of the intensity transmission of the polarizer, resulting in a change in intensity at the photodiode proportional to the voltage across the substrate at the probe point [3].

For frontside probing, suitable for microstrip transmission lines, the fields extend from the conductor roughly the distance of the substrate thickness; the probe spot size is set to approximately one-tenth of the substrate thickness to accurately measure the conductor potential. For backside probing, suitable for planar transmission lines and wire interconnects, the characteristic extent of the fields into the substrate is the distance between the signal conductor and ground; the substrate thickness must be

much greater than the signal-ground spacing (a requirement met by good high-frequency IC design) and the probe beam spot diameter should be less than or equal to the conductor width. An additional requirement on the IC is that the backside of the wafer be sufficiently polished to allow for passage of the probe beam with negligible scattering.

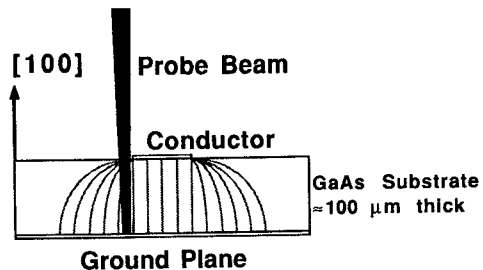


Fig. 1 Frontside probing for microstrip transmission lines. Typical conductor widths are 40-70 μm .

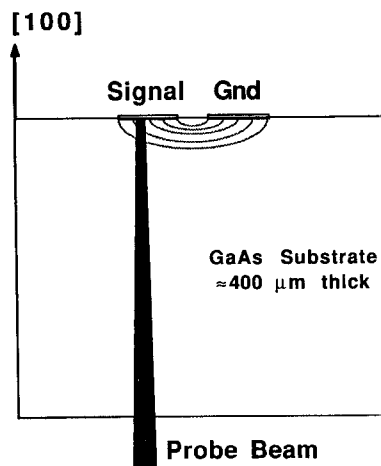


Fig. 2 Backside probing for planar transmission lines and wire interconnects. Conductor widths may be as small as 2 μm .

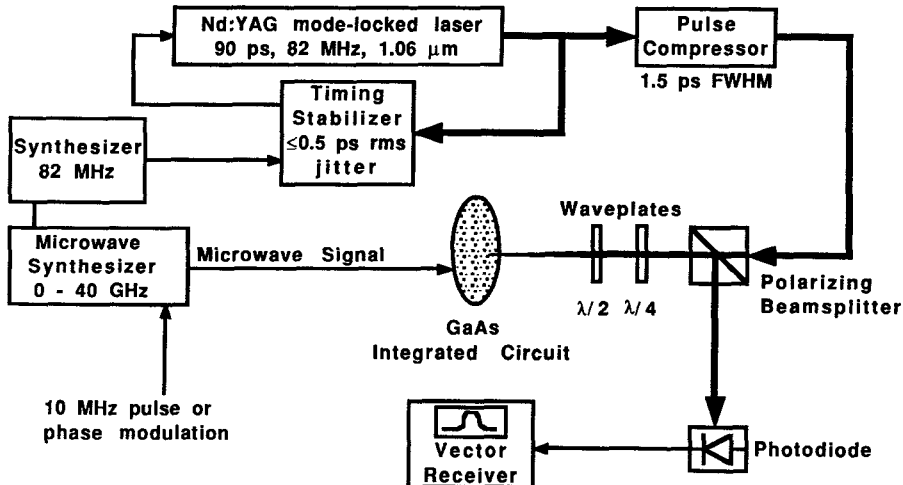


Fig. 3 Electrooptic sampler system

The sampling system is shown schematically in Fig. 3. A commercially available, mode-locked Nd:YAG laser produces 1.06 μm , 90 ps pulses at an 82 MHz rate. The laser has free-running pulse-to-pulse timing fluctuations of 4 ps rms, reduced to less than 300 fs rms by a phase-lock-loop feedback system [4]. A fiber-grating pulse compressor shortens the pulses to 1.5 ps FWHM (full width at half maximum) [5,6]. The beam passes through a polarizing beamsplitter and two waveplates to adjust its polarization, then is focused through the IC substrate with a microscope objective to a 3 μm spot on the probed conductor (backside probing) or a 10 μm spot on the ground plane adjacent to the probed conductor (frontside probing). The reflected light is analyzed by the polarizing beamsplitter; the change in intensity, proportional to the voltage across the GaAs substrate, is detected by a photodiode connected to a vector receiver.

To drive the IC a microwave synthesizer generates either sinusoidal excitation for microwave circuits or the clock or data signals for digital circuits. For wafer-level testing of IC's a microwave probe station (Cascade Microtech Model 42) was modified to allow for backside electrooptic probing. The transmission line probes used with this test station allow for launching a signal on the IC with repeatable, low reflection connections in a 50 Ω environment to 26 GHz. The synthesizer is set to an exact multiple of the laser repetition rate (82 MHz), plus a small frequency offset Δf (1-100 Hz); the resulting intensity modulation at the photodiode receiver varies at this slow offset rate Δf . To enhance the system sensitivity, the synthesizer is also modulated at 10 MHz to allow synchronous detection in a spectral region where laser amplitude noise approaches the shot noise limit.

Measurement bandwidth/time resolution

The system's bandwidth is determined by the optical transit time of the pulse through the GaAs substrate where fields are present, the optical pulsewidth, and pulse-to-pulse timing jitter of the laser with respect to the microwave synthesizer driving the circuit. In general the optical transit time of the pulse in the GaAs substrate can be neglected for microwave IC's. Because the optical and microwave dielectric constant in GaAs are nearly equal, microwave transmission lines have a cutoff frequency for higher-order modes roughly equal the inverse of the optical transit time. Well-designed microwave circuits operate at frequencies well below the multimode cutoff frequency. Only when measuring interconnects near or above the cutoff frequency (where dispersive characteristics are of interest) must the optical transit time be considered. For example, the optical transit

time for a 125 μm thick substrate is 3 ps, corresponding to a 3 dB response rolloff of >100 GHz.

The compressed pulsewidth, 1.5 ps FWHM, is measured with an optical autocorrelator and calculated assuming a gaussian pulseshape. However, a more quantitative estimate of the spectral content of the pulse is determined by numerically Fourier transforming the autocorrelation. This calculation gives the power spectral density of the pulse with no assumption about the pulseshape.

Timing jitter influences both bandwidth and sensitivity; the impulse response of the sampling system is the convolution of the optical pulse with the probability distribution of its arrival time (neglecting optical transit time), while those Fourier components of the jitter lying within the detection bandwidth of the receiver introduce noise proportional to the time derivative of the measured waveform [4]. Stabilization of the laser timing is thus imperative for low-noise measurements of microwave or picosecond signals. To address this issue a timing stabilization feedback system was implemented to reduce the jitter to a level less than the optical pulsewidth. Figure 4 shows the measured phase noise of one harmonic of the laser with an HP 8662 low-phase noise synthesizer as the reference for the feedback system. Integrating the phase noise allows calculation of the jitter in time, less than 300 fs rms.

Measurement sensitivity

To achieve accuracy, repeatability, and fast acquisition of circuit measurements requires shot-noise-limited sensitivity in the detection system [2]. Low-frequency noise on the laser contributes excess amplitude noise above the shot noise limit to a frequencies of several hundred kilohertz. To translate the signal detection to a frequency where this 1/f laser noise is below the shot noise limit, the microwave signal to the IC is modulated at 10 MHz. With a narrowband 10 MHz vector receiver, the resulting shot-noise-limited sensitivity is sufficient to acquire measurements at scan rate of 10-100 Hz with a typical voltage sensitivity of 100-300 $\mu\text{V}/\text{Hz}$. For microwave circuits or simple digital circuits, the input signal is pulse modulated at 10 MHz. For sequential digital circuits which do not operate correctly with chopped excitation, a small-deviation 10 MHz phase modulation is used. In this case the received signal, proportional to the derivative of the sampled waveform, is integrated in software [7].

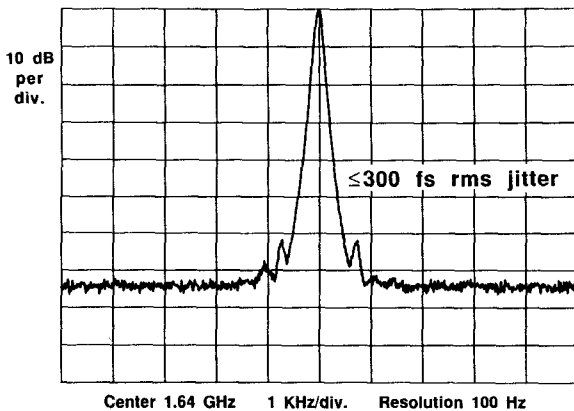


Fig. 4 Laser intensity phase noise at the 20th harmonic of the pulse repetition rate, measured with a photodiode and RF spectrum analyzer. The noise floor of this measurement is instrumentation limited, giving an upper limit for the timing jitter of 300 fs rms.

The pulse compressor is also a source of several types of excess amplitude noise, due to stimulated Raman scattering (SRS) and temperature-induced polarization drift in the non-polarization-preserving fiber [8]. These noise sources are avoided by keeping the optical power in the fiber well below the Raman threshold and by temperature stabilizing the fiber to suppress polarization drift.

Circuit Measurements

Configured as a vector voltmeter, the sampler can measure voltage transfer functions of microwave structures and circuits, including measurements of standing wave ratio, phase velocity, and lateral voltage distribution of microstrip [9] and coplanar waveguide transmission (CPW) lines. On GaAs microwave amplifiers, propagation of microwave signals internal to microstrip and coplanar-waveguide MESFET distributed amplifiers (Fig. 5)[10,11] have been measured.

The sampler measures the standing-wave voltage on a conductor due to the sum of the forward and reverse traveling waves

$$V(z) = V^+ e^{-j\beta z} + V^- e^{+j\beta z}$$

where V^+ and V^- are the forward and reverse traveling coefficients, β is the wavenumber, and z the position. For a one-port transmission line the ratio of the traveling wave coefficients V^+ and V^- is the reflection coefficient Γ , or S_{11} , the insertion loss. To determine this ratio we have measured the voltage as a function of position along the conductor and then numerically fit the data to obtain a minimum mean-square-error estimate of the traveling wave coefficients (Figs. 6 & 7.)

The sampler can also be used as a time-domain instrument to measure internal-node waveforms in the IC. We have measured propagation delays on digital circuits clocked at microwave frequencies such as an 18 GHz static frequency divider (from Hughes Research Labs[12],[13]), gain saturation of distributed amplifiers (from Varian Research[11]), and frequencies to 40 GHz on transmission lines (Fig. 8). This type of time-domain information can be obtained with neither a sampling oscilloscope (due to limited bandwidth) nor a network analyzer (small-signal response only.)

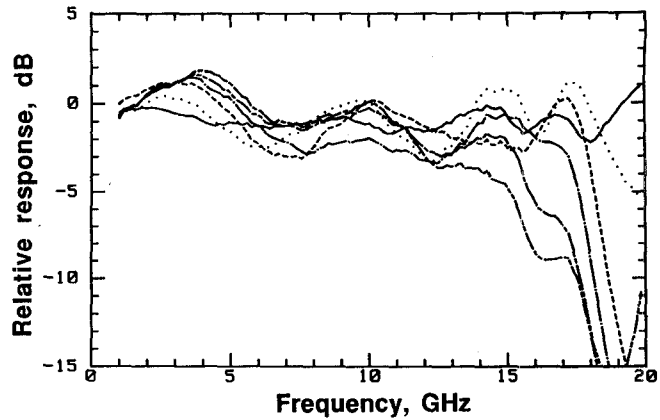


Fig. 5 Frequency response of internal gate nodes and termination in a 5-stage distributed amplifier. The ripple is due to standing waves on the conductor, the rolloff at 18 GHz is due to the cutoff of the periodically loaded gate line, and the droop in the magnitude is loss due to FET input conductance.

Conclusion

With a pulwidth of 1.5 ps FWHM and a timing jitter ≤ 300 fs, the electrooptic sampler has a measurement bandwidth exceeding 100 GHz. A microwave probe station, modified to allow for electrooptic probing of GaAs IC's at the wafer level, has been used to characterization ultrafast digital GaAs IC's clocked at microwave frequencies and microwave IC's such as distributed amplifiers. Directivity for network analyzer type measurements is obtained by scanning the probe along transmission line conductors to calculate the forward and reverse traveling wave coefficients from the voltage standing wave. We have experimentally verified this technique for a one port, terminated transmission line to millimeter-wave frequencies. Extension of this technique to two-port measurements of devices and circuits will allow for full S-parameter measurements with the reference plane on the IC, avoiding complex de-embedding of IC test fixtures.

Acknowledgments

We acknowledge the generous equipment donations of Cascade Microtech, Inc., Tektronix, Inc., and the Hewlett-Packard Co, with specific thanks to Dale Albin from HP for use of the Ka-band frequency doubler. K. Weingarten acknowledges a Newport Research Award and M. Rodwell acknowledges an IBM Pre-doctoral Fellowship. This work was supported in part by the Air Force Office of Scientific Research contract F49620-85K-0016 and by Wright-Patterson Air Force Base Avionics Laboratory contract F33615-86-C-1126.

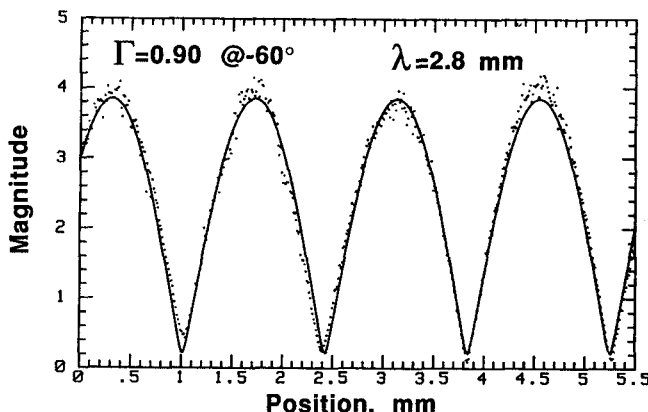


Fig. 6 Magnitude of the voltage standing wave on an open terminated CPW transmission line on GaAs at 40 GHz. The points are data and the solid line is the fitted curve.

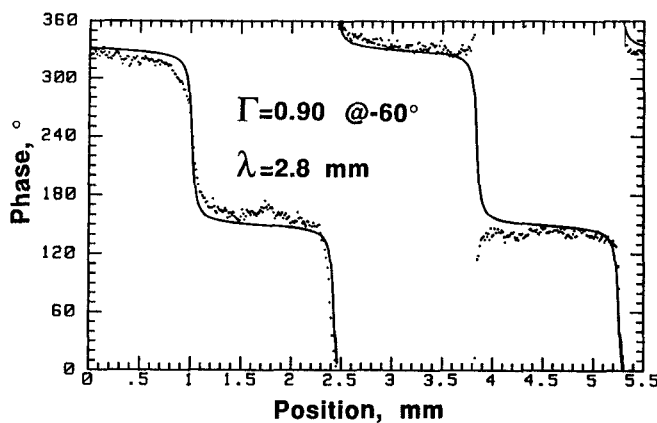


Fig. 7 Phase of the voltage standing wave on an open terminated CPW transmission line on GaAs at 40 GHz. The points are data and the solid line is the fitted curve. Each division of 10° in phase corresponds to 0.7 ps in time.

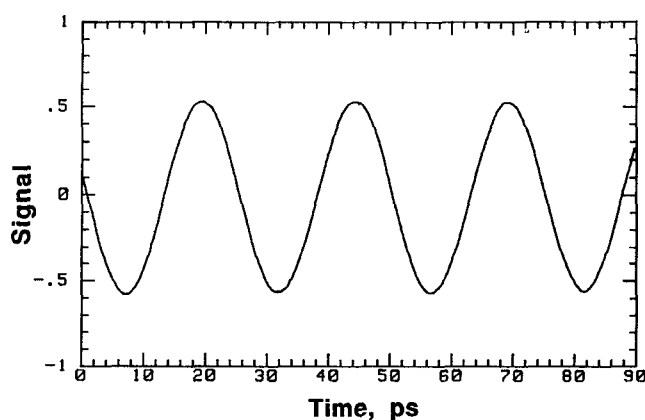


Fig. 8 Time waveform on the CPW line at 40 GHz drive frequency.

References

1. J.A. Valdmanis, G.A. Mourou, and C.W. Gabel: IEEE J. Quant. Elec., **19**, 664 (1983); J.A. Valdmanis and G.A. Mourou: *ibid.*, **22**, 69 (1986)
2. B.H. Kolner and D.M. Bloom: IEEE J. Quant. Elec., **22**, 79, (1986)
3. J.L. Freeman, S.K. Diamond, H. Fong, and D.M. Bloom: Appl. Phys. Lett., **47**, 1083 (1985)
4. M.J.W. Rodwell, K.J. Weingarten, D.M. Bloom, T. Baer, and B.H. Kolner: Optics Letters, **11**, 638, (1986)
5. J.D. Kafka, B.H. Kolner, T. Baer, and D.M. Bloom: Opt. Lett., **9**, 505, (1984)
6. D. Grischkowsky and A.C. Balant: Appl. Phys. Lett., **41**, 1, (1982)
7. M.J.W. Rodwell, K.J. Weingarten, J.L. Freeman, and D.M. Bloom: Electron. Lett., **22**, 499 (1986)
8. K.J. Weingarten, M.J.W. Rodwell, and D.M. Bloom: To appear in Picosecond Electronics and Optoelectronics, (Springer-Verlag, 1987)
9. K.J. Weingarten, M.J.W. Rodwell, J.L. Freeman, S.K. Diamond, and D.M. Bloom: Ultrafast Phenomena V, ed. by G.R. Fleming and A.E. Siegman, Springer Ser. Chem. Phys., Vol. 46 (Springer-Verlag, New York 1986) p. 98
10. M.J.W. Rodwell, M. Riazat, K.J. Weingarten, B.A. Auld, and D.M. Bloom: IEEE Trans. Microwave Theory Tech., MTT-34, 1356, (1986)
11. G. Zdziuk, M. Riazat, R. LaRue, C. Yuen, and S. Bandy: To appear in Picosecond Electronics and Optoelectronics, (Springer-Verlag, 1987)
12. J.F. Jensen, L.G. Salmon, D.S. Deakin, and M.J. Delaney: Technical Digest of the 1986 International Electron Device Meeting, p. 476
13. J.F. Jensen, K.J. Weingarten, D.M. Bloom: To appear in Picosecond Electronics and Optoelectronics, (Springer-Verlag, 1987)